

C.W. Fairall¹, D.E. Wolfe¹, L. Bariteau², S. Pezoa¹, J.E. Hare², R.A. Weller³, E.F. Bradley⁴, J.B. Edson⁵, D. Helmig², W. McGillis⁷, B. Huebert⁷, and B. Blomquist⁷

¹ NOAA Earth System Research Laboratory, Boulder, CO, USA (Chris.Fairall@noaa.gov) / ² University of Colorado, Boulder, CO, USA / ³ Woods Hole Oceanographic Institution, Massachusetts, USA / ⁴ CSIRO, Canberra, Australia / ⁵ University of Connecticut, Groton, Connecticut, USA / ⁶ Lamont-Doherty Earth Observatory of Columbia University, Palisades, New York, USA / ⁷ University of Hawaii, Honolulu, HI, USA

1. Introduction

OceanObs99 envisaged an air-sea flux observing system with research campaigns to improve flux parameterizations and an expansion of direct and autonomous flux measurements. Recent progress includes the deployment of flux reference buoys, development of packages for routine direct measurements of turbulent fluxes, the use of in situ data to validate NWP fluxes, the development of satellite-derived and blended flux products, and specialized validation activities. Flux products are required for forcing ocean models, understanding ocean dynamics, investigating the forcing of variability by the atmosphere and ocean, understanding the ocean's role in climate variability and change, and assessing the realism of data-assimilative ocean models and coupled ocean-atmosphere models used for predictions from weather to climate time scales.

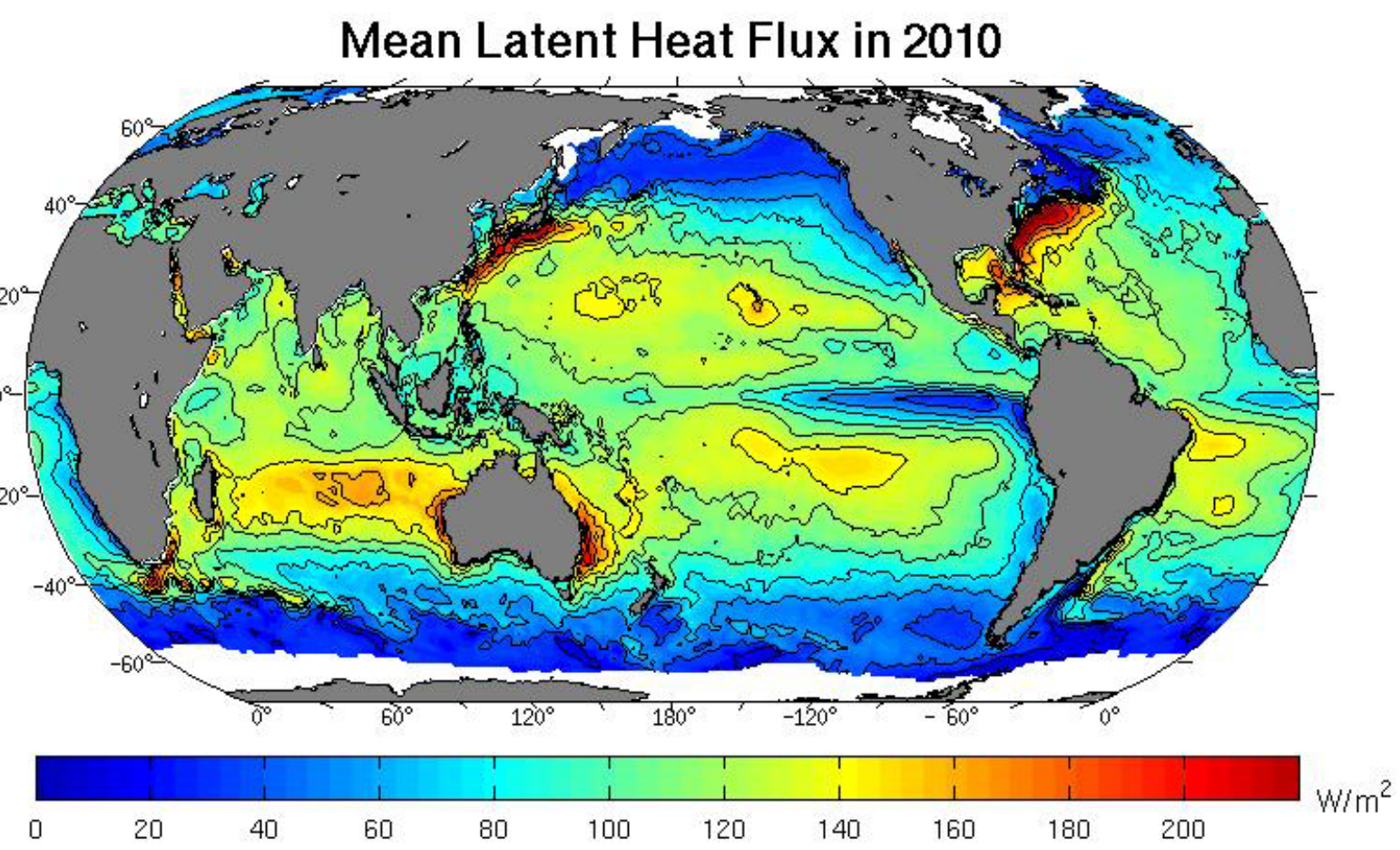


Figure 1. Annual mean (2010) surface latent heat flux from the WHOI OAF flux product (Yu and Weller, 2007).

Direct flux measurements are scarce and cannot be used to generate global flux datasets. Rather the surface fluxes are parameterized in terms of bulk meteorological estimates of the surface atmospheric and oceanic states. These parameterizations are used to compute fluxes from observed variables as well as those used in NWP and reanalyses. This poster considers advances in direct observations of the turbulent fluxes of momentum, sensible and latent heat, and trace gases plus downward surface fluxes of IR and solar radiation at, or near, the ocean surface.

2. Direct observation versus parameterization

Turbulent Fluxes

The vertical flux of some atmospheric constituent, x , can be characterized by the covariance of its fluctuations, x' , with fluctuations in the vertical air motions, w' ,

$$F_x = \overline{w'x'} \quad (1)$$

In this context, x refers to the horizontal components of wind (u, v), air temperature (T), air specific humidity (q), or concentration of a trace gas (c) such as CO_2 , DMS, or Ozone.

Direct observations are obtained by measuring the time series of w' and x' and computing the average covariance. Turbulent fluxes are usually parameterized through the bulk transfer coefficient, C_x

$$\overline{w'x'} = c_x^{-1} c_d^{-1/2} S \Delta X = C_x S \Delta X \quad (2)$$

Here c_x is the bulk transfer coefficient for the variable x (d being used for wind speed) and C_x is the total transfer coefficient; ΔX is the sea-air difference in the mean value of x , and S is the mean wind speed (relative to the ocean surface)

Gas transfer is usually characterized with the transfer velocity, k ,

$$F_x = \alpha k (C_w / \alpha - C_a) = \alpha k \Delta C = \left[\frac{\alpha k}{u_*} \right] u_* \Delta C = C_P u_* \Delta C \quad (3)$$

where k is the transfer velocity, α is dimensionless solubility of the gas in seawater, C_w and C_a the mean concentration of the gas in the water and air. In the final term on the RHS of (3) we separate the flux computation into a chemical factor, C_P , [equivalent of $c_x^{-1/2}$ in (2)] and a physical forcing factor $u_* \Delta C$ [equivalent to $c_x^{-1/2} S \Delta X$ in (2)].

Figure 2. High speed flux sensors on foremast of the NOAA Ship Ronald H. Brown.

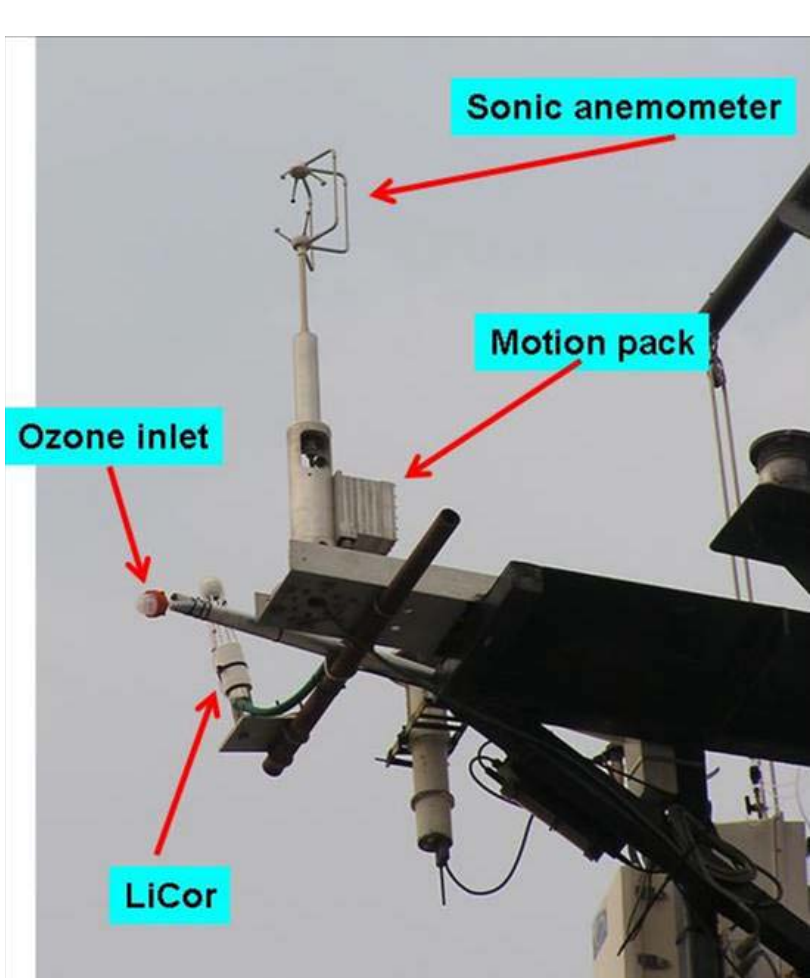


Figure 3. A buoy radiometer assembly. For redundancy there are two Eppley PIRs (reflective domes) and two PSPs (clear domes) mounted on a buoy tower.

Radiative Fluxes

Several technologies are available for direct measurements of radiative fluxes. For sea-going platforms, conventional thermopile-based sensors are used for solar flux (pyranometer) and longwave IR flux (pyrgeometer). Individual units are calibrated against secondary standards in either laboratory or field venues.

Radiative transfer models can be used to compute flux at the surface given a detailed specification of the scattering and absorption properties of the atmospheric column. For surface flux applications, simple parameterizations are available that relate the atmospheric properties to surface variables [see poster by DeSzoeke et al.].

3. Progress on direct flux observation technology

Direct flux measurements from ship became feasible in the early 1990's. Major advances in the accuracy, reliability, and ruggedness of sonic anemometers and the development of commercial fast hygrometers suitable (well, almost suitable) for marine deployments led to more routine application in field programs. Cheaper computers and data acquisition systems coupled with new integrated GPS-inertial motion measurement systems resulted in automated flux systems and allowed deployments on unattended offshore platforms and buoys.



Figure 4. Examples of new platforms being used extensively for direct flux observations.

Progress on observations of direct fluxes of air-sea transfer of trace gases has been dependent on the development of fast sensors for the gases. Recent examples for marine applications are CO_2 , DMS, and ozone. The requirement for high speed and high resolution has proven extremely demanding (see discussion in Rowe et al. 2011).

Considerable progress was made with improving accuracy for the simple pyrgeometer measurement of IR flux (Fairall et al. 1998). Ship-buoy intercomparisons and improvements in low voltage datalogging technology now allow observations of IR flux that are accurate to within 5 W/m^2 from ships and buoys (Weller et al. 2008). The most significant advance in solar flux sensors is improved accuracy based on using quartz windows, improved engineering, and carefully determined temperature corrections. This has led to more accurate cosine response. Figure 5 shows an example comparing older and newer technology. On a cloud-free day, the Eppley unit would overestimate the daily-averaged flux by about 1.5%. We have also developed pitch-roll stabilized mounts for the radiometers to eliminate pitch and roll induced errors.

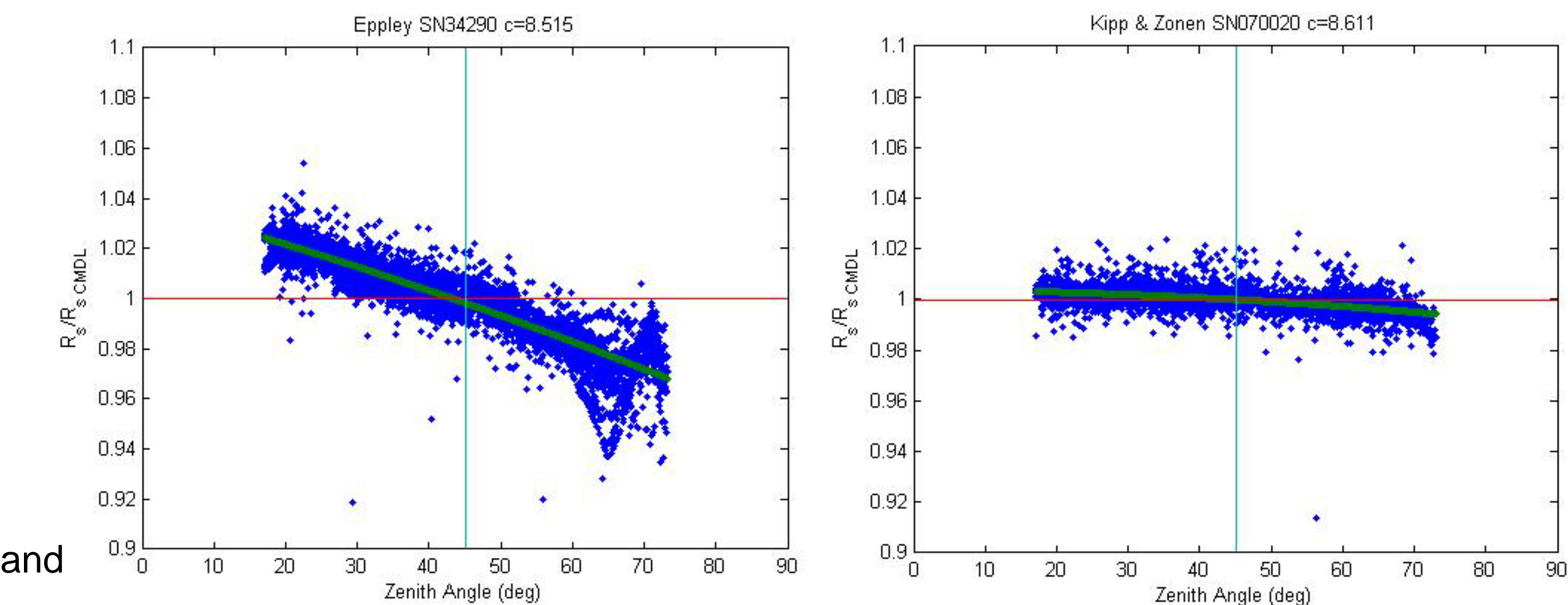


Figure 5. Direct calibration of pyranometers at the NOAA GMD facility in Boulder, CO. Solar flux is determined as the sum of direct and diffuse components. The pyranometer calibration coefficient is defined so that the solar flux is correct at a zenith angle of 45 deg. This figure shows the ratio of the pyranometer output normalized by the directly measured value as a function of zenith angle on a clear day. The unit on the left is from Eppley Laboratories; the unit on the right is from Kipp and Zonen.

4. Intensive field programs and extended monitoring

In this research we use different types of observations for instrument development or characterization, to support intensive field programs, and in so-called extended monitoring programs where measurements are made on annual cruises to the same locations (usually to service buoys). These observations form a flux data base that has been used to improve flux parameterizations. In Table 1 we list components of the PSD/UConn meteorological flux database. Table 2 lists observations used in a recent synthesis of gas transfer fluxes (Fairall et al. 2011). The extended monitoring fluxes also form a database that can be used to compare global flux products and/or NWP and climate models (see the poster by DeSzoeke et al.).

Region	Designation	Reference
Multiple	12 open ocean cruises 1991-1999	Fairall et al. [2003]
Equatorial E. Pac	12 PACS cruises 1999-2004	Fairall et al. [2008]
Coast E. US	NEAQS	Fairall et al. [2006]
Atlantic Trade Wind	RICO	Rauber et al. [2007]
Chilean stratus region	9 VOCALS synthesis cruises 2001-2010	DeSzoeke et al. [2011]
Coastal N. Atlantic	CBLAST Platform 2001-2003	Edson et al. [2007]
N. Atlantic	CLIMODE 2006-2007	Marshall et al. [2009]

Year	Algorithm	Reference
1996	COARE2.5	Fairall et al. [1996a,b]
2000	COAREG2.5_CO2	Fairall et al. [2000]; Hare et al. [2004]
2003	COARE3.0	Fairall et al. [2003]
2004	COAREG3.0_DMS	Blomquist et al. [2006]
2006	COAREG3.0_Ozone	Fairall et al. [2007]
2008	PCBs, PCDEs	Perlinger and Rowe [2008]
2010	79 Gases	Johnson [2010]; Rowe et al. [2011]
2011	COAREG3.1 CO2, DMS, Ozone, SF6, He	Fairall et al. [2011]

Table 1. Momentum and heat flux observations by covariance methods used in this project.

Table 3. History of the COARE algorithms. The terminology COARE.N.M refers to publically available versions of the meteorological flux algorithm.

Table 2. Ocean trace gas flux observations by covariance methods; *indicates data used in this paper.

Gas	Designation	Reference
CO2	Gasex98 and Methods*	McGillis et al. [2001a,b]
	Gasex01*	McGillis et al. [2004]
	Methods	Miller et al. [2010]
	Methods	Prytherch et al. [2010]
	N. Atlantic	Lauvset et al. [2011]
DMS	SO GasEx*	Edson et al. [2011]
	SE Pacific*	Huebert et al. [2004]
	N. Atlantic and SE Pacific*	Blomquist et al. [2006]
	N. Pacific*	Marandino et al. [2007]
	S. Pacific*	Marandino et al. [2009]
Ozone	Methods*	Blomquist et al. [2010]
	Gulf Mexico	Grachev et al. [2011]
	Five Regions*	Helmig et al. [2011]

5. State-of-the-art turbulent flux parameterizations

This the authors of this poster maintain a community bulk turbulent flux algorithm known as COARE. COARE originally was applicable to momentum, sensible, and latent heat fluxes and then extended for application to trace gases (currently usable for 79 gases). See Table 3 for a historical summary. Recently (Fairall et al. 2011), COARE3.0 was compared with a collection of nearly 26,700 observations of drag and heat transfer coefficients (from three independent research groups). The algorithm agreed overall within 5% with observations averaged in wind speed bins over a 10-m neutral wind speed range of 2 to 18 ms^{-1} (see Fig. 6). Observations of gas transfer k for CO_2 and DMS were normalized to a fixed Schmidt number of 660 (equivalent to that for CO_2 at 20 C). Using an ensemble of gas flux observations from 6 research groups and 9 field programs; mean k_{660} values in 10-m neutral wind speed bins were computed. A reasonable fit of the mean k_{660} vs U_{10m} values was obtained for both CO_2 and DMS with a version of COAREG3.1 using tangential friction velocity, u_* , in the non-bubble term with the turbulent/molecular coefficient $A=1.6$ and the bubble-mediated coefficient $B=1.8$ (Figs. 7). Work is underway on an update (COARE4.0) that will include observations from the UConn database of FLIP, buoy, and platform observations. The remarkable agreement between the measurements and the algorithm is demonstrated in the comparison of observations from the CLIMODE buoy shown in Fig. 8.

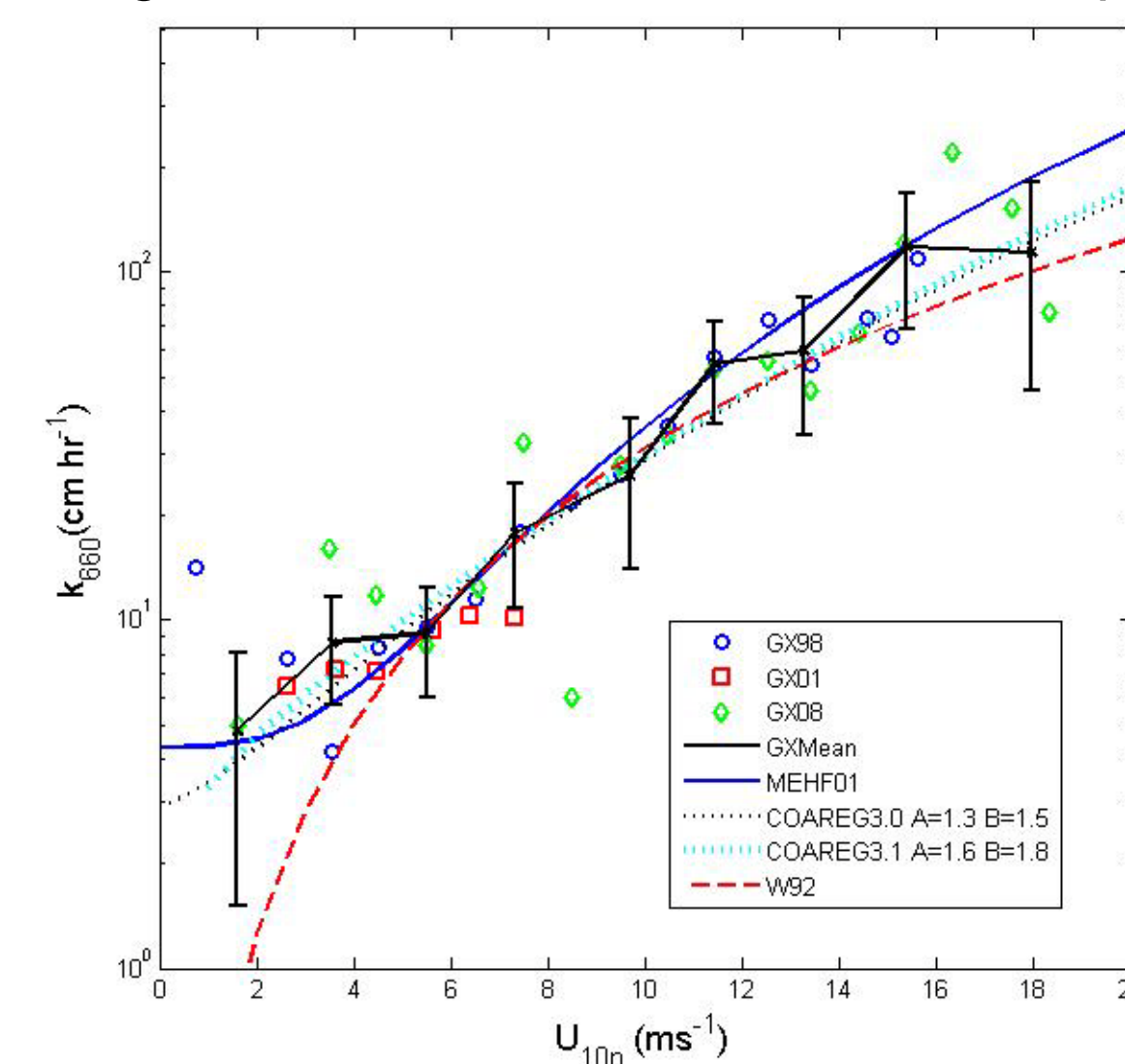


Figure 7a. Gas transfer coefficient for CO_2 as a function of 10-m neutral wind speed from direct surface-based observations. The black line is the mean of the data sets; the error bars are statistical estimates of the uncertainty in the mean. Symbols are: circle - GASEX98, square - GASEX01, diamond - SOGASEX08. The parameterizations shown are: blue solid line - McGillis et al. [2001a]; black dotted line - COARE3.0G CO_2 ; cyan dotted line - COARE3.1G CO_2 using u_* ; red dashed line - W92 [Wanninkhoff 1992].

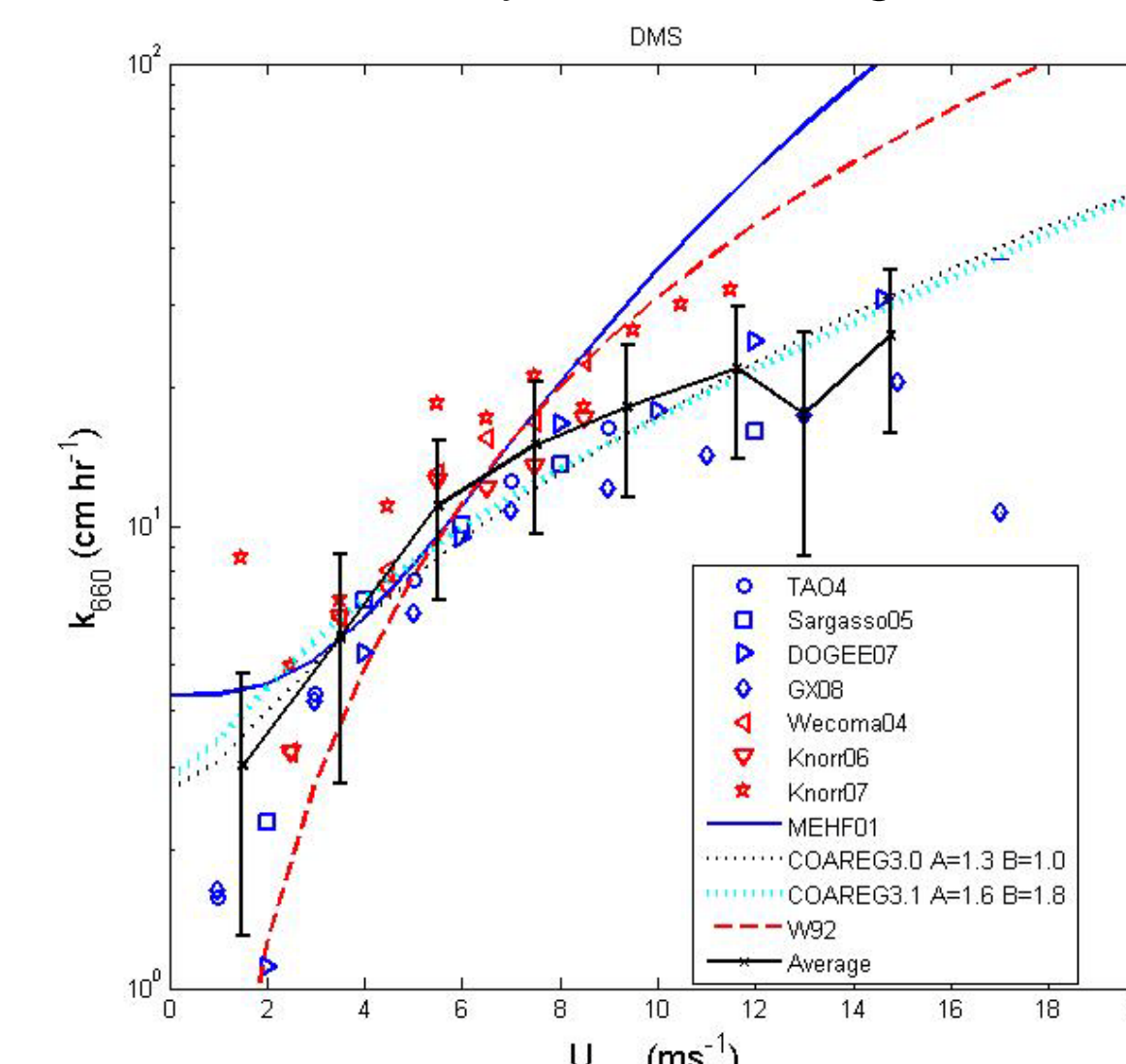


Figure 7b. DMS gas transfer coefficient as a function of 10-m neutral wind speed from direct surface-based observations. The black line is the mean of the data sets; the error bars are statistical estimates of the uncertainty in the mean. Symbols are: circle - TAO04 (Equatorial Pacific); square - Sargasso Sea 05, right triangle - DOGEE07, diamond - SOGASEX08, left triangle - Wecoma04, down triangle - Knorr06, pentagon - Knorr07. The parameterizations shown are: blue solid line - McGillis et al. [2001], black dotted line - COARE3.0G DMS; cyan dotted line - COARE3.1G DMS using u_* ; red dashed line - W92.

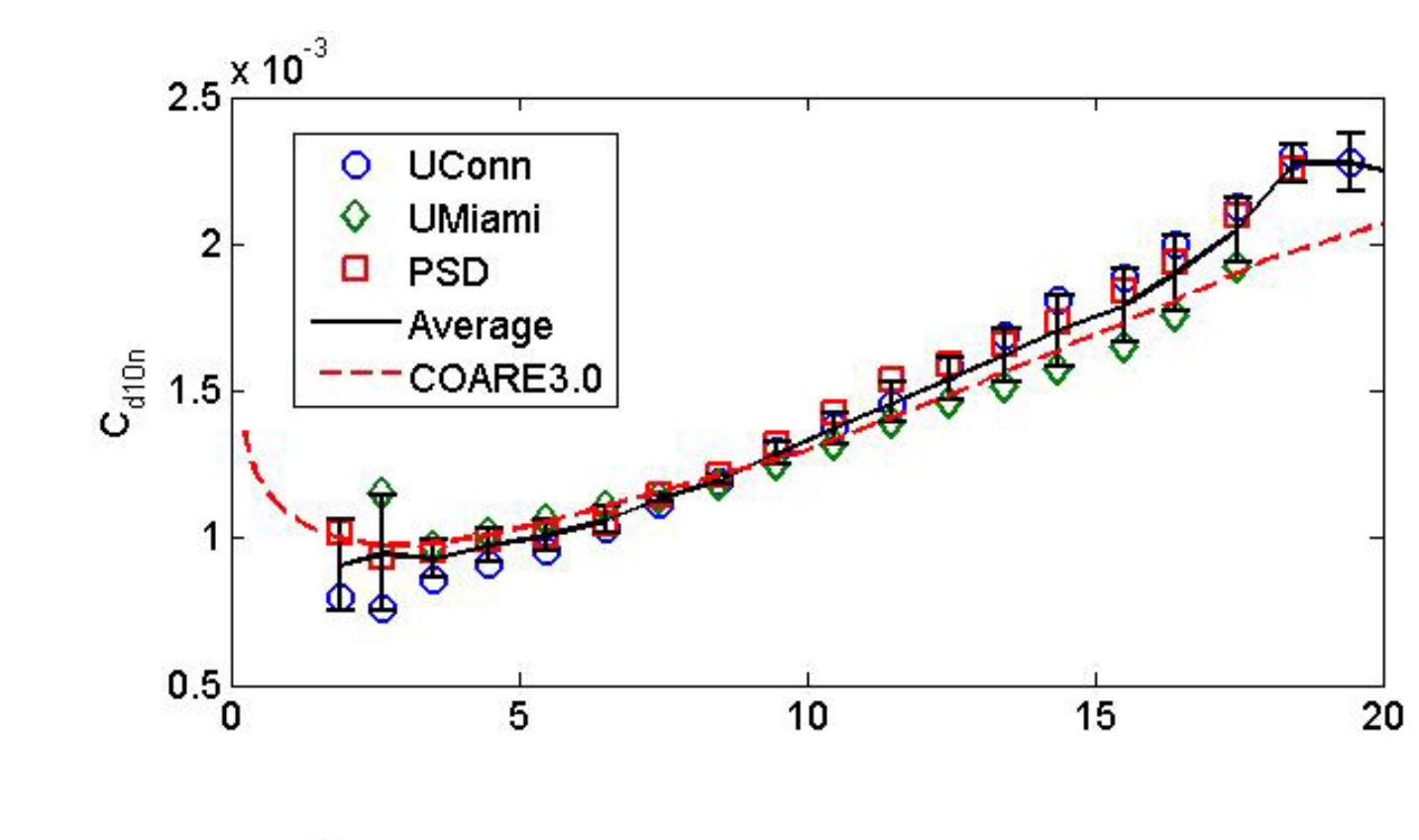


Figure 6. 10-m neutral turbulent transfer coefficients as a function of 10-m neutral wind speed from direct surface-based observations. Symbols are: circle - U. Connecticut (FLIP, Martha's Vineyard Observatory, and moored buoys), diamond - U. Miami (ASIS spar buoy), and square - NOAA/ESRL/PSD (ships). Upper panel: C_{10m} ; Lower panel: C_{E10m} (ESRL/PSD) and C_{H10m} (U. Connecticut). The black line is the mean of the data sets; the error bars are statistical estimates of the uncertainty in the mean.

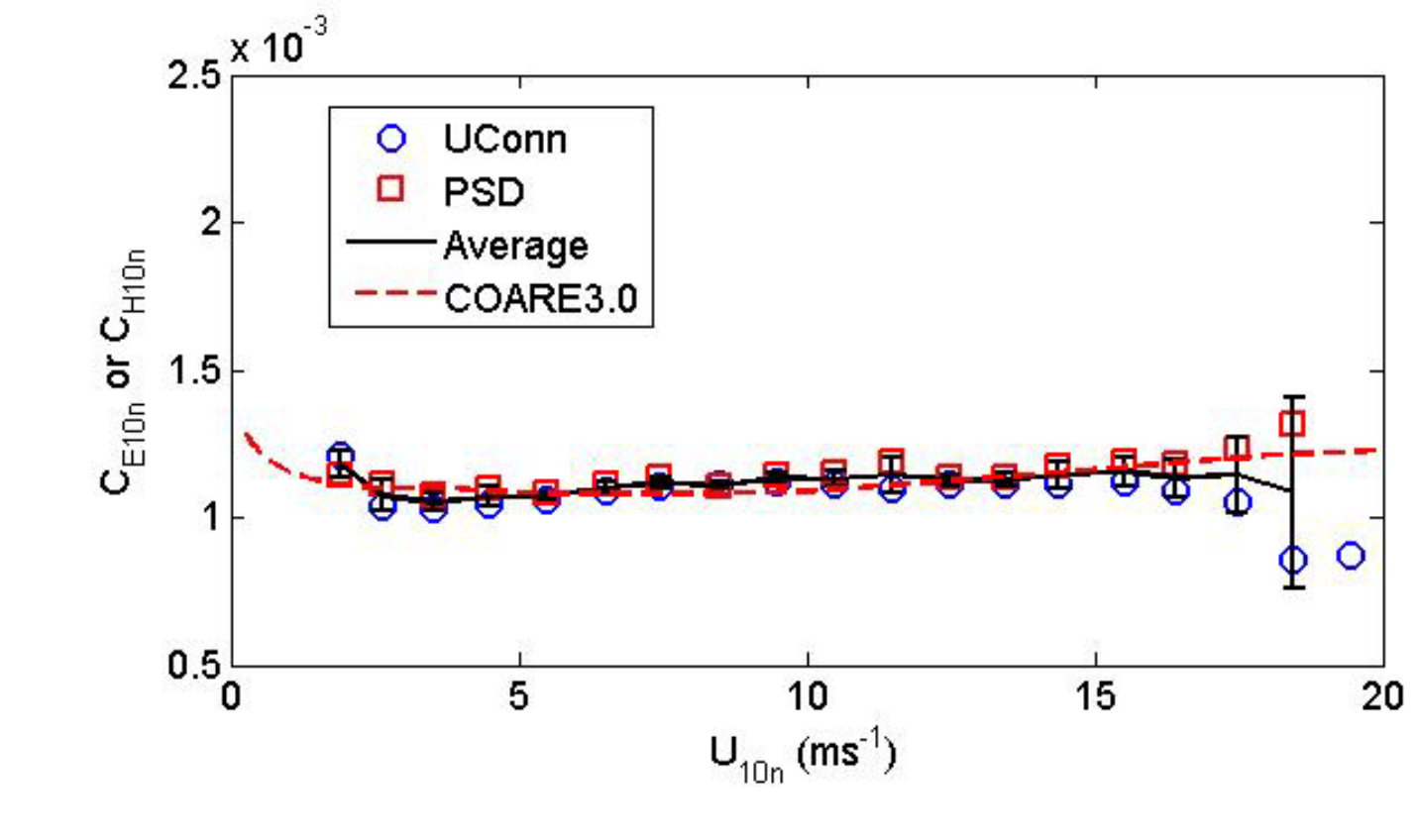


Figure 8. Sample time series of turbulent fluxes (momentum, upper; buoyancy, lower) from the University of Connecticut buoy-mounted direct covariance observation system. This example is from the CLIMODE deployment in the N. Atlantic; the sensor is 5-m above the sea surface. Fluxes shown are the direct covariance (DC) measurements, COARE version 3.0, and COARE version 4.0 (recently tuned to the UConn database). Time resolution is 30-min.